On the generation of waves by turbulent wind

By O. M. PHILLIPS
St. John's College, Cambridge

(*Received* 18 *February* 1957)

CONTENTS

SUMMARY

A theory is initiated for the generation of waves upon a water surface, originally at rest, by a random distribution of normal pressure associated with the onset of a turbulent wind. Correlations between air and water motions are neglected and the water is assumed to be inviscid, so that the motion of the water, starting from rest, is irrotational. It is found that waves develop most rapidly by means of a resonance mechanism which occurs when a component of the surface pressure distribution moves at the same speed as the free surface wave with the same wavenumber.

The development of the waves is conveniently considered in two stages, in which the time elapsed is respectively less or greater than the time of development of the pressure fluctuations. An expression is given for the wave spectrum in the initial stage of development (§ 3.2), and it is shown that the most prominent waves are ripples of wavelength $\lambda_{cr} = 1{\cdot}7$ cm, corresponding to the minimum phase velocity $c = (4gT/\rho)^{1/4}$ and moving in directions $\cos^{-1}(c/U_c)$ to that of the mean wind, where U_c is the 'convection velocity' of the surface pressure fluctuations of length scale λ_{cr} or approximately the mean wind speed at a height λ_{cr} above the surface. Observations by Roll (1951) have shown the existence under appropriate conditions, of waves qualitatively similar to those predicted by the theory.

Most of the growth of gravity waves occurs in the second, or principal stage of development, which continues until the waves grow so high that non-linear effects become important. An expression for the wave spectrum is derived (§ 4.1), from which follows the result

$$\overline{\xi^2} \sim \frac{\overline{p^2} t}{2\sqrt{2}\rho^2 U_c g},$$

where $\overline{\xi^2}$ is the mean square surface displacement, $\overline{p^2}$ the mean square turbulent pressure on the water surface, t the elapsed time, U_c the convection speed of the surface pressure fluctuations, and ρ the water density. This prediction is consistent with published oceanographic measurements (§ 4.3).

It is suggested that this resonance mechanism is more effective than those suggested by Jeffreys (1924, 1925) and Eckart (1953), and may provide the principal means whereby energy is transferred from the wind to the waves.

1. Introduction

In the following pages, a theory is proposed to account for the generation of waves by wind. The problem has attracted attention for many years, during which time many experimental studies have been made and many hypotheses advanced to account for the results of these observations. However, no really satisfactory explanation of the phenomenon has been offered and not even the physical processes involved can be regarded as known. Although casual observations of wind-generated waves must have been made by almost everyone, thorough experimental investigations are difficult, and our understanding of the subject has consequently been very limited. The best known of the various hypotheses put forward are those due to Jeffreys (1924, 1925) and Sverdrup & Munk (1947), which are described in a valuable review of the subject by Ursell (1956). Jeffreys's sheltering hypothesis is the very reasonable one that the wind passing over any waves already existing on the surface induces a variable pressure distribution, and that the component which is in phase with the wave slope supplies further energy to the wave, resulting in its continued development. The predictions from this hypothesis involve a sheltering coefficient s, which, for a wave in which the energy gain from the wind just balances the viscous dissipation, is required to have a value of approximately 0·27. However, experimental measurements of s made on solid wave models gave values which were smaller by an order of magnitude, so that it must be concluded that the effect of sheltering, though undoubtedly present to some degree, is not efficient enough to account for the observed wave growth. The failure of this hypothesis led Sverdrup & Munk and others to consider the effect of the tangential stresses set up on the water surface. By assuming that *all* the energy communicated to the water by these stresses appears in waves and none in currents, they were able to account for the order of

magnitude of the observed wave heights. But such theories, based upon energy considerations alone, are hardly satisfactory; and, as a means of producing the irrotational motion associated with surface waves, the shear stresses seem intuitively to be singularly inefficient, particularly in the early stages of wave growth. It seems more plausible to suppose that the initiation and early development of waves is a consequence of fluctuations in the normal pressure upon the surface, which under natural conditions are always present on account of the invariably turbulent character of the wind. As the waves develop, the influence of the shear stresses upon the wave pattern may not remain negligible, though it is difficult to give an *a priori* estimate of their importance. However, it will be seen later that the observed wave heights can be explained in terms of the pressure fluctuations alone, so that it seems possible that the effects of the shear stresses are rarely, under natural conditions, dominant in the wave growth.

The present approach is developed without specific empirical assumptions, such as the sheltering hypothesis of Jeffreys or the assumptions of energy transfer involved in the work of Sverdrup & Munk. The mathematical problem can be formulated as follows. Given that at an initial instant a turbulent wind commences to blow across an infinite sheet of deep (inviscid) water originally at rest, generating a distribution of fluctuating pressure on the surface which is a stationary random function of position and time, the aim is to study the properties of the surface displacement at subsequent times.

An attempt to solve the problem in a manner similar to this was made by Eckart (1953). He represented the pressure distribution associated with the turbulent wind in a very specific way, i.e. as an aggregate of pressure points of a given size and duration over a finite storm area. It is very likely that this representation is too specific to give an adequate description of the randomness of the fluctuations in pressure associated with the turbulent wind. It will be seen later that this randomness is essential, since the water surface selects from the whole range of wave-numbers in the applied pressure distribution certain ones whose amplitude increases most rapidly by a mechanism involving a type of resonance. The inadequacy of Eckart's representation in this respect is probably the most important cause of the failure of his theory to explain the observed wave heights; his predicted values are an order of magnitude too small.

It is clear from the way the problem has been formulated that the present treatment is not a stability theory, such as the Kelvin–Helmholtz model (see, for example, Ursell 1956). It is found that waves can grow not only through an instability but by this mechanism of resonance between the components of the surface pressure distribution and the free surface waves. It cannot be claimed that this resonance effect, whose nature will be explained more fully below, is the only one capable of generating waves; for instabilities of the Kelvin–Helmholtz type will almost certainly occur if the wind velocity is sufficiently high and established sufficiently rapidly (perhaps producing the capillary ripples observed in strong gusts of wind),

and in some circumstances the effects of sheltering and shear-stress action may not be negligible. However, it does account in a natural way for a variety of observed phenomena, though a true appreciation of its scope and limitations must await the results of further investigations, particularly on the effects of the non-linearities which become important when the wave slopes become appreciable.

My understanding of the problems involved in the generation of waves by wind has been greatly helped by discussions with Dr M. S. Longuet-Higgins of the National Institute of Oceanography, Surrey, and with Mr F. Ursell and Dr A. A. Townsend at Cambridge; it is a pleasure to acknowledge my indebtedness to them for their constructive comments upon this work.

2. The approach to the problem

2.1. *The physical background*

It is a matter of common observation that winds, blowing over the ground or over water, do not consist of streams of air in steady and uniform motion but rather of an irregular series of 'puffs' and 'lulls' carrying eddies and swirls distributed in a disordered manner. In the language of the fluid dynamicist, the wind is not laminar, but invariably turbulent. This turbulent nature of the wind will be found to result in the birth and growth of waves upon a water surface. The atmospheric eddies, or random velocity fluctuations in the air, are associated with random stress fluctuations on the surface, both pressures (i.e. normal stresses) and tangential shear stresses. The eddies are borne forward by the mean velocity of the wind, and at the same time they develop, interact and decay, so that the associated stress distribution f both moves across the surface with a certain convection velocity dependent upon the velocity of the wind and evolves in time as it does so. An overall convection velocity of the stress fluctuations can be defined mathematically as *the velocity of the frame of reference in which their frequency scale is least*, or their time scale greatest. This least frequency scale is characteristic of the evolution of the stress distribution, whereas the frequencies observed, say at a fixed point, are invariably greater because of added contributions from the sweeping of the stress pattern past the point.

The stress distribution contains components with a very large range of wave-numbers, and as might be expected, Fourier components with very different wave-numbers $\boldsymbol{\kappa}$ are convected at different speeds. The surface stress fluctuations of any given length scale can be attributed to turbulent eddies near the surface whose length scale is of the same order of magnitude, and the larger eddies will be convected by the mean wind with a greater speed than the smaller stress-generating eddies lying near the surface. A definition to express this slightly more refined concept can be given as follows. If $F(\boldsymbol{\kappa}, t)$ is the two-dimensional spatial Fourier transform of the surface stress covariance $\overline{f(\mathbf{x}', t')f(\mathbf{x}' + \mathbf{x}, t' + t)}$, then the convection velocity

$\mathbf{U}_c(\boldsymbol{\varkappa})$ for the components of wave-number $\boldsymbol{\varkappa}$ is the velocity of the frame of reference in which the time scale

$$[F(\boldsymbol{\varkappa}, 0)]^{-1} \int_0^\infty F(\boldsymbol{\varkappa}, t)\, dt$$

is greatest. That is, we take axes moving with velocity $\mathbf{u}$, and in this frame of reference (see § 4.1)

$$F(\boldsymbol{\varkappa}, t, \mathbf{u}) = [F(\boldsymbol{\varkappa}, t)]_{\mathbf{u}=0} \cos(\boldsymbol{\varkappa} . \mathbf{u}\, t).$$

The convection velocity $\mathbf{U}_c(\boldsymbol{\varkappa})$ is the value of $\mathbf{u}$ for which

$$\int_0^\infty [F(\boldsymbol{\varkappa}, t)]_{\mathbf{u}=0} \cos(\boldsymbol{\varkappa} . \mathbf{u}\, t)\, dt$$

is a maximum. This maximum time scale, or development time of the stress fluctuations, which appears later in the analysis, will be denoted by $\Theta(\boldsymbol{\varkappa})$. In the frame of reference convected with velocity $\mathbf{U}_c$, the time dependence is slowest and is determined by the growth and decay of the eddies as they are carried along.

The convection velocity $\mathbf{U}_c$ defined in this way must be related to the mean velocity of the wind measured at a certain height above the surface. The physical picture of the convection of the stress-generating eddies mentioned above suggests that $\mathbf{U}_c(\boldsymbol{\varkappa})$ is of the same order as the mean velocity of the wind at a height κ^{-1} above the surface. Now, the mean velocity profile of the wind $U(z)$ is determined by the friction velocity u_* $(=(\tau_0/\rho_a)^{1/2}$ where τ_0 is the mean horizontal shear stress at the surface, and ρ_a the density of the air), by the roughness length z_0, and by the kinematic viscosity ν, and is of the form

$$\frac{U(z)}{u_*} = 2{\cdot}3\left[\log\frac{z}{z_0} + B\left(\frac{u_* z_0}{\nu}\right)\right]. \tag{2.1}$$

In aerodynamically rough flow, the function B is in effect zero, and the roughness length z_0 for a water surface is probably related to u_* by an expression of the type $u_*^2 \propto g z_0$ and for moderate winds is of order 0·1 cm. The velocity profile of the wind over a water surface is discussed in recent review articles by Ellison (1956) and Ursell (1956); the reader is referred to these accounts if further detail is required. However, the important point in this connection is that when z/z_0 is large, the variation of mean velocity with height is slow, so that for the components of the stress distribution whose length scale is of the order of several metres, the convection velocity $U_c(\boldsymbol{\varkappa})$ is very nearly equal to the wind velocity as usually measured from a ship. For the very much smaller components, however, it may be considerably less.

Our problem is to discover the nature of the action between this stress distribution and the water surface, and the investigation of this is described in the following sections. However, it will perhaps be clearer if some of the

salient features are described first in physical terms, although this will necessitate anticipation of some of the analysis to be developed later. This background will, it is hoped, make the direction and implications of the subsequent mathematics more evident.

We have assumed that the fluctuating pressure upon the water surface is responsible for the birth and early growth of waves. If a Fourier analysis were to be made in the two space dimensions of the surface and in time, components would be found over a wide range of wave-numbers and frequencies. These components of the pressure fluctuations acting upon the surface generate small forced oscillations, and the amplitude of any Fourier component of the surface displacement depends upon the amplitude of the corresponding component of the forcing pressure fluctuations. But the response of the water surface to the various Fourier components of the pressure field is not uniform, since certain combinations of wave-number and frequency in the components of the surface displacement are excited more readily than others. In particular, if the pressure distribution contains components whose wave-numbers and frequencies coincide with possible modes of *free* surface waves, then a type of resonance occurs, and the continued presence of these components in the pressure distribution (although their amplitudes may not be large) generates surface waves whose amplitude continually increases.

The nature of this resonance can be seen most clearly by considering the motion in a frame of reference moving with the convection velocity of the surface pressure distribution. Suppose we can, for the moment, neglect the evolution of the pattern of stress fluctuations so that the distribution is stationary in the convected frame of reference. The various components generate wavelets of small amplitude which propagate along the surface in all directions; but for a given convection velocity (provided it is not too small) there are two particular wave modes that propagate in the direction of the wind at the convection velocity. These particular wavelets remain stationary with respect to the pressure distribution which produced them. The phase difference between these particular wavelets and the Fourier component of the pressure field with the same wave-number remains fixed, so that the conditions which gave them birth remain to ensure their continued growth.

But this is an over-simplification, because the evolution of the stress pattern usually cannot be ignored. If we make a two-dimensional spatial Fourier analysis of the surface pressure distribution with respect to axes moving with the convection velocity, the amplitude and phase of each component varies slowly in a random manner with time. The particular wavelet which is stationary with respect to the convected reference frame is still subject to a pressure component of the same wave-number, but one whose phase now wanders and whose amplitude varies. However, the average amplitude of the wavelet continues to increase, although we should expect the variation of mean square amplitude at this wave-number to be slower than it would be if the phase were constant. This process of

statistical development through a random influence is already familiar in the contexts of diffusion and random-walk problems.

The mathematical problem in which this process appears has already been formulated in the previous section, and certain assumptions will now be made to facilitate the analysis. We should like to be able to assume that the statistical properties of the applied pressure fluctuations are independent of the waves already generated. We will therefore endeavour to determine the conditions under which this is likely to be true. Initially the water is at rest, so that in the very early stages of wave growth (i.e. the 'initial stage' of § 3) this assumption can clearly be made as a first approximation, since the initial pattern of ripples has not yet grown large enough in amplitude to have a significant effect on the wind. Presumably, however, the pattern of ripples soon reaches some sort of statistical equilibrium, and there is evidence (see Ursell 1956, p. 240) that the roughness length z_0 of the surface is determined by these short steep ripples rather than by the height of the longer waves that subsequently develop. It seems, then, that after quite a short duration these ripples begin to exercise a profound influence upon the mean velocity profile and the other mean properties of the turbulent wind. However, a much greater time is taken for the development of the longer gravity waves in which we are more interested. It seems, therefore, that when the duration is sufficiently long, the components of the pressure distribution generating the longer *gravity* waves are independent of the waves of this kind already present. To summarize, this assumption seems justified under two sets of conditions: (i) when the duration of the wind is very small, and (ii) for gravity waves when the duration is large. In both cases, this assumption must be expected to fail when the wave steepness becomes too great, since, for example, sheltering effects may then become important.

As a further simplification, the viscosity of the water will be neglected, since it is probably unimportant for all but the shortest waves over moderate intervals of time. The motion, which is envisaged as starting from rest, is then irrotational. Consideration is restricted to waves whose mean-square slope is small, so that the surface boundary condition can be linearized. Finally, for definiteness and convenience, the surface pressure fluctuations are assumed to be statistically homogeneous over regions of the surface whose extent is comparable with the correlation areas of the atmospheric turbulence, and, after the initial instant, to be statistically steady.

2.2. *The equations of motion*

In this problem it is convenient to express the surface pressure fluctuations and surface displacements in terms of their Fourier components. The pressure fluctuation p and displacement ξ are stationary random functions of position $\mathbf{x} = (x_1, x_2)$ in the surface plane, so that simple Fourier transforms do not exist. However, we can invoke a more effective technique, used widely in the theory of random functions (see, for example, its application

to turbulence theory in Batchelor (1953)), by defining the Fourier–Stieltjes transform

$$\xi(\mathbf{x}, t) = \int dA(\boldsymbol{\kappa}, t) e^{i\boldsymbol{\kappa}\cdot\mathbf{x}}, \tag{2.2}$$

where the integration is over all wave-numbers $\boldsymbol{\kappa}$ in the plane. The two-dimensional instantaneous spectrum of the surface displacement is the Fourier transform of the covariance

$$\Xi(\mathbf{r}) = \overline{\xi(\mathbf{x})\xi(\mathbf{x}+\mathbf{r})},$$

which decreases to zero rapidly as $|\mathbf{r}| \to \infty$, so that its Fourier transform

$$\Phi(\boldsymbol{\kappa}) = (2\pi)^{-2} \int \Xi(\mathbf{r}) e^{-i\boldsymbol{\kappa}\cdot\mathbf{r}}\, d\mathbf{r},$$

where $d\mathbf{r}$ represents $dr_1\, dr_2$ and the integration is over the entire surface with $\mathbf{x}$ fixed, does exist in the ordinary sense. From the inverse of this relation, it can be shown that the spectrum is given in terms of the Fourier–Stieltjes transform by

$$\Phi(\boldsymbol{\kappa}, t) = \frac{\overline{dA(\boldsymbol{\kappa}, t)\, dA^*(\boldsymbol{\kappa}, t)}}{d\kappa_1\, d\kappa_2}, \tag{2.3}$$

where the asterisk indicates the complex conjugate. Similar expressions can be written down to specify the pressure fluctuations on the surface. The two-dimensional Fourier–Stieltjes transform

$$p(\mathbf{x}, t) = \int d\varpi(\boldsymbol{\kappa}, t) e^{i\boldsymbol{\kappa}\cdot\mathbf{x}} \tag{2.4}$$

is related to the spectrum function $\Pi(\boldsymbol{\kappa}, t)$ of the surface pressure fluctuations by the expression

$$\begin{aligned}\Pi(\boldsymbol{\kappa}, t) &= (2\pi)^{-2} \int \overline{p(\mathbf{x}, t')p(\mathbf{x}+\mathbf{r}, t'+t)}\, e^{-i\boldsymbol{\kappa}\cdot\mathbf{r}}\, d\mathbf{r}, \\ &= \frac{\overline{d\varpi(\boldsymbol{\kappa}, t')\, d\varpi^*(\boldsymbol{\kappa}, t'+t)}}{d\kappa_1\, d\kappa_2},\end{aligned} \tag{2.5}$$

which is a function of the wave-number $\boldsymbol{\kappa}$ and time separation t.

The motion in the water has been assumed to be irrotational, so that a potential ϕ can be defined such that

$$\mathbf{u} = \nabla\phi \quad \text{and} \quad \nabla^2\phi = 0, \tag{2.6}$$

where $\mathbf{u}$ is the velocity vector. The surface boundary condition for waves of infinitesimal height is

$$\frac{1}{\rho}\left\{p - T\left(\frac{\partial^2\xi}{\partial x_1^2} + \frac{\partial^2\xi}{\partial x_2^2}\right)\right\} = \left[\frac{\partial\phi}{\partial t}\right]_{z=0} - g\xi, \tag{2.7}$$

where ρ is the density of the water, T the surface tension at the interface, g the gravitational acceleration, ξ the surface displacement, and z is the vertical position coordinate to be measured downwards from the undisturbed

surface level. It is convenient to express this equation in a frame of reference moving with an arbitrary velocity U, and it becomes

$$\frac{p}{\rho} = \left[\frac{\partial\phi}{\partial t} - U_i\frac{\partial\phi}{\partial x_i}\right]_{z=0} - g\xi + \frac{T}{\rho}\left(\frac{\partial^2\xi}{\partial x_1^2} + \frac{\partial^2\xi}{\partial x_2^2}\right). \tag{2.8}$$

The normal velocity of the surface is $d\xi/dt$, or in the moving frame of reference,

$$\left(\frac{\partial}{\partial t} - U_i\frac{\partial}{\partial x_i}\right)\xi = \left[\frac{\partial\phi}{\partial z}\right]_{z=0} = \int (dA' - i\boldsymbol{\kappa}.\mathbf{U}\,dA)e^{i\boldsymbol{\kappa}.\mathbf{x}}, \tag{2.9}$$

where the representation (2.1) is used, and where the accent represents time differentiation in the convected frame of reference. The irrotational motion in the water is specified by the solution of $\nabla^2\phi = 0$ with the boundary conditions that $\phi \to 0$ as $z \to \infty$, and that at $z = 0$, $\partial\phi/\partial z$ is as given by (2.9). This solution is (see Phillips 1955)

$$\phi = -\int \frac{dA' - i\boldsymbol{\kappa}.\mathbf{U}\,dA}{\kappa} e^{-\kappa z}e^{i\boldsymbol{\kappa}.\mathbf{x}}, \tag{2.10}$$

where $\kappa = |\boldsymbol{\kappa}|$. The equation (2.8) can now be expressed in terms of the Fourier–Stieltjes transforms as

$$\frac{d\varpi}{\rho} = -\left[\frac{\partial}{\partial t} - i\boldsymbol{\kappa}.\mathbf{U}\right]^2\frac{dA}{\kappa} - g\,dA - \frac{T}{\rho}\kappa^2\,dA, \tag{2.11}$$

or

$$dA'' - 2in_1\,dA' - (n_1^2 - n_2^2)\,dA = -\frac{\kappa}{\rho}d\varpi(t), \tag{2.12}$$

where

$$n_1 = \boldsymbol{\kappa}.\mathbf{U} = \kappa U\cos\alpha, \qquad n_2 = (g\kappa + T\kappa^3/\rho)^{1/2}. \tag{2.13}$$

Equation (2.12) describes the growth of each component of the surface displacement in terms of the corresponding component of the pressure distribution. If we now specify U as the convection velocity of the component of the pressure field of wave-number $\boldsymbol{\kappa}$, the quantity n_1 represents the frequency, in radians per second, of a wave with wave-number κ and speed $\mathbf{U}.\boldsymbol{\kappa}/\kappa = U_c\cos\alpha$ in a direction at an angle α to that of the wind, and n_2 is the frequency of free surface waves of wavelength $2\pi/\kappa$.

The fundamental equation (2.12) specifies the development with time of the Fourier–Stieltjes transform $dA(\boldsymbol{\kappa}, t)$ of the surface displacement in terms of the transform $d\varpi(\boldsymbol{\kappa}, t)$ of the pressure fluctuations, which is, after the initial instant, a stationary random function of time. Its solution, subject to the initial conditions appropriate to an undisturbed surface at rest, namely $dA = dA' = 0$ at $t = 0$, can be expressed as

$$dA(\boldsymbol{\kappa}, t) = \frac{e^{i(n_1+n_2)t}}{2in_2}\int_0^t \frac{\kappa}{\rho}d\varpi(\tau)\exp\{-i(n_1+n_2)\tau\}\,d\tau - \\ - \frac{e^{i(n_1-n_2)t}}{2in_2}\int_0^t \frac{\kappa}{\rho}d\varpi(\tau)\exp\{-i(n_1-n_2)\tau\}\,d\tau,$$

or

$$dA(\boldsymbol{\kappa}, t) = \frac{i\kappa}{2\rho n_2}\int_0^t d\varpi(\tau)[\exp\{-i(n_1-n_2)(\tau-t)\} - \\ - \exp\{-i(n_1+n_2)(\tau-t)\}]\,d\tau. \tag{2.14}$$

This solution provides the common starting point for the investigations of the next two parts of this paper. It illustrates how the amplitude of each Fourier–Stieltjes component of the wave pattern is dependent upon the history of the applied pressure distribution from the initial instant $t = 0$. The development of each component of the wave field falls naturally into two stages: the intial stage over values of time $t \ll \Theta(\boldsymbol{\kappa})$ (i.e. the development time of the fluctuations in pressure of wave-number $\boldsymbol{\kappa}$, or the time scale of $d\varpi(\boldsymbol{\kappa}, t)$ in the convected frame of reference), and the second or principal stage of development for which $t \gg \Theta$ and during which most of the growth of gravity waves takes place. The properties of the waves in each of these stages will be discussed in turn.

3. The initial stage of wave development

3.1. *The initial response of the water surface*

We define the initial stage of development as the period of time for which $t \ll \Theta(\boldsymbol{\kappa})$, so that over this range of t, $d\varpi(\boldsymbol{\kappa}, t)$ in the convected frame of reference varies little from its value at the initial instant. In the integration of the general solution (2.14), $d\varpi(\boldsymbol{\kappa})$ can be considered independent of time, and the solution becomes

$$dA(\boldsymbol{\kappa}, t) \doteq \frac{i\kappa\, d\varpi(\boldsymbol{\kappa})}{2\rho n_2}\int_0^t \left(\exp\{-i(n_1-n_2)(\tau-t)\}-\exp\{-i(n_1+n_2)(\tau-t)\}\right) d\tau,$$

$$= \frac{\kappa\, d\varpi(\boldsymbol{\kappa})}{\rho(n_1^2-n_2^2)}\left\{1-\frac{n_1+n_2}{2n_2}\exp\{-i(n_1-n_2)t\}+\right.$$

$$\left.+\frac{n_1-n_2}{2n_2}\exp\{-i(n_1+n_2)t\}\right\}. \quad (3.1)$$

From this, there follows a relation between the wave spectral function $\Phi(\boldsymbol{\kappa})$ and the two-dimensional, simultaneous pressure spectrum $\Pi(\boldsymbol{\kappa}) \equiv \Pi(\boldsymbol{\kappa}, 0)$; for

$$dA^*(\boldsymbol{\kappa}, t) \doteq \frac{\kappa\, d\varpi^*(\boldsymbol{\kappa})}{\rho(n_1^2-n_2^2)}\left\{1-\frac{n_1+n_2}{2n_2}\exp\{i(n_1-n_2)t\}+\frac{n_1-n_2}{2n_2}\exp\{i(n_1+n_2)t\}\right\},$$

and since

$$\Phi(\boldsymbol{\kappa}) = \frac{\overline{dA(\boldsymbol{\kappa})\, dA^*(\boldsymbol{\kappa})}}{d\kappa_1\, d\kappa_2}, \qquad \Pi(\boldsymbol{\kappa}) = \frac{\overline{d\varpi(\boldsymbol{\kappa})\, d\varpi^*(\boldsymbol{\kappa})}}{d\kappa_1\, d\kappa_2},$$

we have

$$\Phi(\boldsymbol{\kappa}, t) \doteq \frac{\kappa^2\Pi(\boldsymbol{\kappa})}{\rho^2(n_1^2-n_2^2)^2}\left\{\frac{3}{2}+\frac{n_1^2}{2n_2^2}-\frac{n_1+n_2}{n_2}\cos(n_1-n_2)t+\frac{n_1-n_2}{n_2}\cos(n_1+n_2)t-\right.$$

$$\left.-\frac{n_1^2-n_2^2}{2n_2^2}\cos 2n_2 t\right\}. \quad (3.2)$$

If we write

$$\nu_1 = n_1 t = \kappa t U_c \cos\alpha, \qquad \nu_2 = n_2 t = (g\kappa + T\kappa^3/\rho)^{1/2} t, \quad (3.3)$$

a dimensionless response factor can be defined as

$$\Gamma = (\nu_1^2-\nu_2^2)^{-2}\left\{\frac{3}{2}+\frac{\nu_1^2}{2\nu_2^2}-\frac{\nu_1+\nu_2}{\nu_2}\cos(\nu_1-\nu_2)+\frac{\nu_1-\nu_2}{\nu_2}\cos(\nu_1+\nu_2)-\right.$$
$$\left.-\frac{\nu_1^2-\nu_2^2}{2\nu_2^2}\cos 2\nu_2\right\}, \quad (3.4)$$

so that the wave spectrum can be expressed in the form

$$\Phi(\boldsymbol{\kappa}, t) \doteqdot \Gamma\kappa^2\Pi(\boldsymbol{\kappa})t^4/\rho^2. \quad (3.5)$$

The function $\Phi(\boldsymbol{\kappa}, t)$ is therefore determined, when $t \ll \Theta(\boldsymbol{\kappa})$, jointly by the spectrum of the imposed pressure fluctuations $\Pi(\boldsymbol{\kappa})$ and by the response factor Γ, itself a function of κ through ν_1 and ν_2, and of t; the balance between these two factors must always be taken into account in considering the wave generation in the initial stage. The function $\kappa^2\Pi(\boldsymbol{\kappa})$ has its maximum when κ is large, of the same order as the wave-numbers associated with the dissipating eddies in the atmospheric turbulence. A brief examination of (3.4) suffices to show that in the (ν_1, ν_2)-plane, Γ is large near the line $\nu_1 = \nu_2$ and in regions where ν_1/ν_2 is large.

Wave-numbers of the first class, for which $\nu_1 \doteqdot \nu_2$, are such that the convection velocity of the pressure distribution is equal to the velocity of free waves with these wave-numbers in the direction of convection; for, from (3.3),

$$U_c\cos\alpha = (g/\kappa + T\kappa/\rho)^{1/2} = c(\kappa). \quad (3.6)$$

Because of the factor $\kappa^2\Pi(\boldsymbol{\kappa})$, the amplitude of these waves is significant only when κ is large (i.e. the wavelength λ is small), which in turn implies, from (3.6), that $U_c\cos\alpha$ should also be small. Waves, or perhaps more properly ripples, of this type are generated immediately after the onset of a gust of sufficient strength. Their direction and speed is such that they remain in phase with the applied pressure distribution during this initial period, developing by the simple resonance mechanism described in § 2.1. These waves can conveniently be called ' resonance waves'. Wave-numbers of the second class, for which $\nu_1 \gg \nu_2$, are associated with the *forced* oscillations of the water surface produced by the pressure fluctuations, and it will be shown later that their amplitude does not increase with time t beyond a small upper bound.

3.2. *Resonance waves*

A simple approximation to the response factor (3.4) when $\nu_1 \doteqdot \nu_2$ can be found in the following manner. Let

$$\chi = \nu_1 - \nu_2; \quad (3.7)$$

and, on substituting this into (3.4), we have

$$\Gamma = (2\nu_2+\chi)^{-2}\chi^{-2}\left\{\frac{3}{2}+\frac{\nu_2^2+2\nu_2\chi+\chi^2}{2\nu_2^2}-\frac{2\nu_2+\chi}{\nu_2}\cos\chi+\frac{\chi}{\nu_2}\cos(2\nu_2+\chi)-\right.$$
$$\left.-\frac{\chi(2\nu_2+\chi)}{2\nu_2^2}\cos 2\nu_2\right\},$$
$$= \frac{1}{2\nu_2^2}\left\{\frac{1-\cos\chi}{\chi^2}+O\left(\frac{\chi}{\nu_2}\right)\right\}.$$

If $\nu_2 \gg 1$, that is, if $t \gg n_2^{-1}$ or $(2\pi)^{-1}$ times the period of free waves of wave-number κ, the second term is negligible and the wave spectrum is given approximately by

$$\Phi(\boldsymbol{\kappa}, t) \doteqdot \frac{\kappa^2 \Pi(\boldsymbol{\kappa}) t^2}{2\rho^2 n_2^2} \frac{1-\cos\chi}{\chi^2} \tag{3.8}$$

when $n_2^{-1} \ll t \ll \Theta$ and $n_1 \doteqdot n_2$.

The existence of a range of values of t satisfying this condition clearly requires that n_2^{-1} is less by one or two orders of magnitude than Θ. Since $n_1 \doteqdot n_2$ for resonance waves, an equivalent statement is that the wavelength λ of the surface disturbance is very much less than the distance travelled by the convected pressure distribution in the time Θ. This condition is likely to be satisfied best when λ is small, in the range corresponding to ripples and short gravity waves. (If, for example, $\Theta(\boldsymbol{\kappa})$ is of the same order as the time scale of the eddies of wave-number κ in the equilibrium range, then the condition can be expressed as

$$\lambda = 2\pi/\kappa \ll U_c \Theta \sim U_c \epsilon^{-1/3} \kappa^{-2/3}$$

(where ϵ is the rate of energy dissipation) or $\kappa \gg 8\pi^3 \epsilon / U_c^3$.)

The wave-number κ in any direction α for which $\Phi(\boldsymbol{\kappa})$ is a maximum is determined by the equation $\chi = 0$, or, from (3.3),

$$T\kappa^2/\rho - \kappa U_c^2 \cos^2\alpha + g = 0, \tag{3.9}$$

which, for each value of $U_c \cos\alpha$ above a certain minimum, gives two resonant wave-numbers, one corresponding to a gravity wave and one to a capillary wave. This is illustrated in figure 1. The solid curve $c(\kappa)$ gives the speed of free surface waves as a function of wave-number κ and the broken line $U_c(\kappa)$ a typical convection speed of the components of the pressure field of wave-number κ, which, as we have seen earlier, is a function which may decrease slowly as κ increases. The exact shape of $U_c(\kappa)$ depends upon the surface roughness, and the curve in figure 1 is for illustrative purposes only. In the direction $\alpha = 0$, that of the convection velocity, resonance waves occur near the wave-numbers such that $U_c(\kappa) = c(\kappa)$, given in figure 1 by the points A and B. As α increases, since the condition for resonance waves is that $U_c(\kappa)\cos\alpha = c(\kappa)$, the resonance wave-numbers are found by translating the dashed curve downwards, and the intersections of the two curves approach each other until at a certain critical angle α_{cr} they coincide. For values of α greater than α_{cr}, no resonance waves are possible. If, as one might expect under normal atmospheric conditions and with an 'aerodynamically-smooth surface' appropriate to the initial period of development, the dependence of U_c upon κ is not very rapid except when κ is large (of order unity), the coincidence point will occur near or a little to the right of G in this diagram, which marks the minimum velocity of free waves under the influence of both gravity and surface tension. It can readily be established from (3.6) that this minimum velocity is given by

$$c_{\min} = (4gT/\rho)^{1/4}, \tag{3.10}$$

so that the wavelength of the critical waves is approximately

$$\lambda_{cr} \doteqdot 2\pi(T/\rho g)^{1/2}. \tag{3.11}$$

The critical angle α_{cr}, i.e. the maximum angle from the direction of the wind at which resonance waves are generated, is given by

$$\alpha_{cr} \doteqdot \cos^{-1}(c_{min}/U_c) = \cos^{-1}(4gT/\rho U_c^4)^{1/4}, \tag{3.12}$$

where U_c is the convection velocity of the wave-numbers κ, i.e. the mean wind velocity at a height of approximately κ^{-1}. Taking the values for water: $\rho = 1\,\mathrm{gm\,cm^{-3}}$, $T = 73\,\mathrm{gm\,sec^2}$, and taking $g = 980\,\mathrm{cm\,sec^{-2}}$, we have $c_{min} = 23\,\mathrm{cm\,sec^{-1}}$ and the critical wavelength $\lambda_{cr} = 2\pi/\kappa_{cr} = 1{\cdot}7\,\mathrm{cm}$.

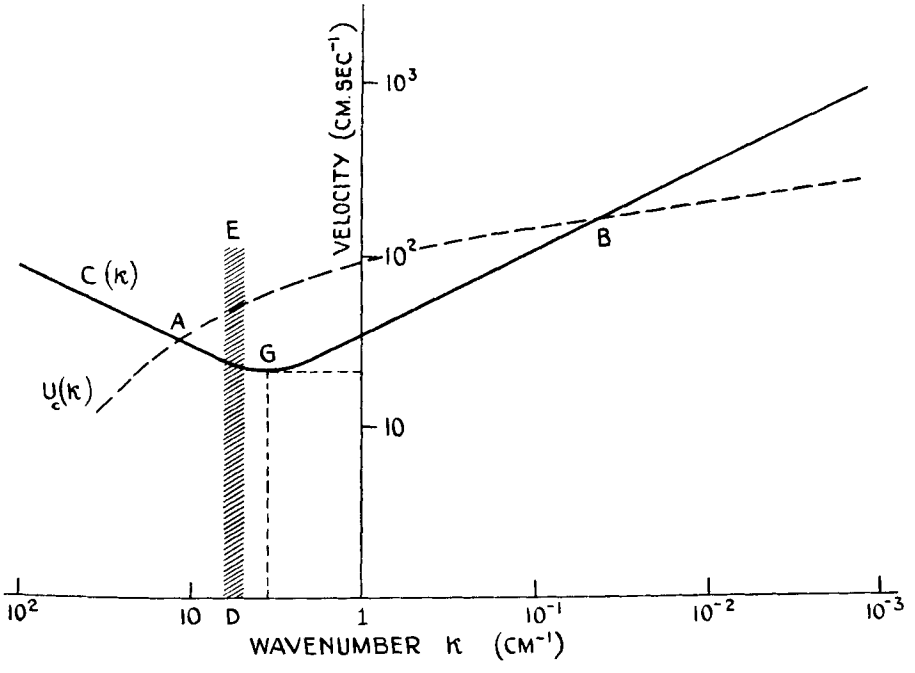

Figure 1.

Of these possible resonance waves, not all may be excited, since for some wave-numbers $\kappa^2\Pi(\boldsymbol{\kappa})$ may be negligible. It is well known that in turbulent flow there is a certain maximum wave-number κ_{max} of the velocity fluctuations, or minimum eddy size, which depends upon the rate of kinetic energy dissipation per unit volume in the flow near the surface and upon the kinematic viscosity ν of the fluid. If the mean velocity gradient is not too large, $\kappa_{max} \sim (\epsilon/\nu^3)^{1/4}$. The surface pressure fluctuations will also have a minimum scale, or maximum wave-number, of the same order of magnitude, so that for values of κ greater than κ_{max}, $\Pi(\boldsymbol{\kappa})$ is negligible. Not a great deal of relevant experimental information is available concerning the magnitude of ϵ under the conditions with which we are concerned, but for a mean wind speed of order $1\,\mathrm{m\,sec^{-1}}$ at a height of

1 metre, a rough estimate guided by experiments such as those of Taylor (1952) suggests that the maximum value of κ is of the order of 10 cm^{-1} or less. Thus, in figure 1, only those wave-numbers below a band such as DE are excited. In the direction $\alpha = 0$, running before the wind, the only resonance waves that occur are the gravity waves corresponding to the point B; the wavelength of the capillary waves given by the point A is too small for excitation to occur. Even if the turbulence were more vigorous, with a smaller minimum eddy size, the growth of the very short capillary waves is hindered by direct viscous dissipation which becomes important for very short wavelengths. Under the conditions illustrated in this figure, no true capillary waves at all would be generated, the smallest wavelengths being little less than λ_{cr}.

It will now be shown that the angle α_{cr} is associated with limiting behaviour in yet another respect. Not only does it represent the maximum angle from the wind direction at which resonance waves can be generated, but also it is found that the amplitude of waves moving in this direction is greater than those in other directions with $\alpha < \alpha_{cr}$. The curve $\chi = 0$ gives the locus of the points in the wave-number plane for which the maximum amplification of resonance waves can occur, and for a given value of U_c is of the form shown in figure 2, where the 1-direction is taken as that of the wind. For angles $\alpha > \alpha_{cr}$ there are no resonance waves, and for angles $\alpha < \alpha_{cr}$ there are two *possible* values of κ for which resonance may occur, although one may not be excited if the minimum scale of the turbulence is too large. The maximum wave-numbers that occur in the surface pressure distribution can be represented by the arc AB, and only the wave-numbers near the curve $\chi(\boldsymbol{\kappa}) = 0$ and within the sector OAB (and its mirror image in OA) will be excited as resonance waves. The width of the resonance band is, as (3.8) shows, determined by the range of values of χ for which $(1-\cos\chi)/\chi^2$ is significant. The limits of this range can conveniently be taken as $\chi(\boldsymbol{\kappa}) = \pm 2\pi$, where, from (3.7),

$$\chi(\boldsymbol{\kappa}) = t\{\kappa U_c \cos\alpha - (g\kappa + T\kappa^3/\rho)^{1/2}\}, \tag{3.13}$$

and these limits, when $n_2 t \gg 1$, are illustrated by the dotted lines in figure 2. It can be shown from (3.13) that the thickness $\Delta\kappa$ of the resonance band at the wave-number κ is such that $|\Delta\boldsymbol{\kappa}| \ll \kappa$ when $t \gg n_2^{-1}$ and decreases as t^{-1}. As time goes on, the range of excited wave-numbers near the curve $\chi(\boldsymbol{\kappa}) = 0$ becomes narrower and narrower while the magnitude of the wave spectral function $\Phi(\boldsymbol{\kappa})$ along this curve rapidly increases.

Now the mean-square surface displacement is given by

$$\overline{\xi^2} = \int \Phi(\boldsymbol{\kappa})\, d\boldsymbol{\kappa}, \tag{3.14}$$

the integration being over the whole $\boldsymbol{\kappa}$-plane. But the integrand is significant only in the part of the strip near the curve $\chi(\boldsymbol{\kappa}) = 0$ lying within the quadrant OAB. A simple and useful approximation to the integral can be obtained by taking locally orthogonal coordinates s, being the distance along the curve $\chi(\boldsymbol{\kappa}) = 0$ from the point D, and χ specifying the

distance normal to the curve. Since the effective width of the resonance band is small, the Jacobian in the expression

$$\xi^2 = \iint \Phi(\mathbf{x})\kappa \, d\kappa d\alpha = \iint \Phi(\mathbf{x})\kappa \frac{\partial(\kappa, \alpha)}{\partial(\chi, s)} d\chi ds \tag{3.15}$$

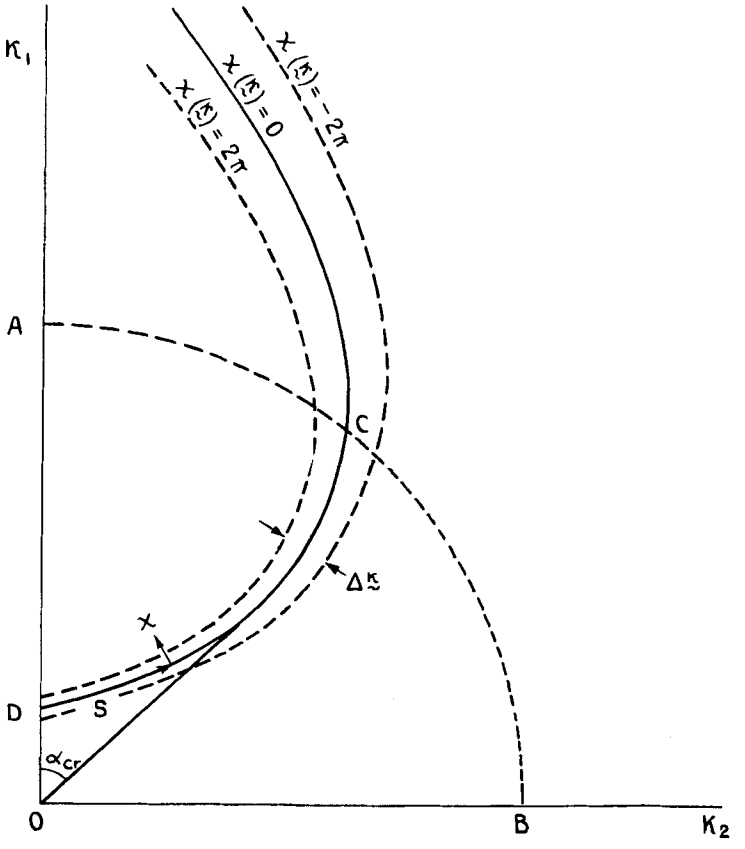

Figure 2.

can be evaluated along $\chi = 0$. The limits of integration of χ can be taken as $\pm \infty$. From (3.13), it can be shown that, when $\chi = 0$,

$$\left.\begin{aligned} \frac{\partial \kappa}{\partial \chi} &= \frac{2\kappa U_c \cos\alpha}{t(g - T\kappa^2/\rho)}, & \frac{\partial \alpha}{\partial \chi} &= -\frac{1}{t\kappa U_c \sin\alpha}, \\ \frac{\partial \kappa}{\partial s} &= \frac{\kappa U_c^2 \sin 2\alpha}{\mathscr{D}}, & \frac{\partial \kappa}{\partial s} &= \frac{g - T\kappa^2/\rho}{\kappa \mathscr{D}}, \end{aligned}\right\} \tag{3.16}$$

where $\mathscr{D}^2 = (\kappa U_c^2 \sin 2\alpha)^2 + (g - T\kappa^2/\rho)^2$, so that

$$\left[\frac{\partial(\kappa, \alpha)}{\partial(\chi, s)}\right]_{\chi = 0} = \frac{4U_c \cos\alpha}{t\mathscr{D}}.$$

The contribution to the mean-square surface displacement per unit length of the resonance band is simply

$$\int_{-\infty}^{\infty} \Phi(\boldsymbol{\kappa})\kappa\left[\frac{\partial(\kappa,\alpha)}{\partial(\chi,s)}\right]_{\chi=0} d\chi \doteq \frac{2\kappa\Pi(\boldsymbol{\kappa})t}{\rho^2 U_c \mathscr{D}\cos\alpha}\int_{-\infty}^{\infty}\frac{1-\cos\chi}{\chi^2}\,d\chi,$$
$$= \frac{2\pi.\kappa\Pi(\boldsymbol{\kappa}).t}{\rho^2 U_c \mathscr{D}\cos\alpha},$$

and the contribution per unit angle in the wave-number plane, or the directional distribution of wave amplitude in the physical plane, is found by multiplying this expression by $\partial s/\partial\alpha$. With the aid of (3.16), this gives

$$\Psi(\alpha) = \frac{2\pi.\kappa^2\Pi(\boldsymbol{\kappa}).t}{\rho^2 U_c\cos\alpha(g - T\kappa^2/\rho)}, \tag{3.17}$$

where κ and α are related by $\kappa U_c\cos\alpha = (g\kappa + T\kappa^3/\rho)^{1/2}$.

From this result, (3.17), most of the important properties of resonance waves in the initial stage can be found immediately. In directions $\alpha \ll \alpha_{cr}$ the resonant wave-number $\kappa \ll \kappa_{cr} = (\rho g/T)^{1/2}$, so that (3.17) becomes approximately

$$\Psi(\alpha) = \frac{2\pi\kappa^2\Pi(\boldsymbol{\kappa})t}{\rho^2 g U_c\cos\alpha}. \tag{3.18}$$

However, as $\kappa \to \kappa_{cr}$, $T\kappa^2/\rho \to g$, and from (3.17), the directional distribution function $\Psi(\alpha)$ becomes infinite at α_{cr}. When $(\kappa_{cr}-\kappa)$ is small, (3.17) gives

$$\Psi(\alpha) \doteq \frac{\pi\kappa^2\Pi(\boldsymbol{\kappa})t}{\rho^2 U_c\cos\alpha}\left(\frac{\rho}{gT}\right)^{1/2}(\kappa_{cr}-\kappa)^{-1}.$$

But from (3.13), on the curve $\chi = 0$ near α_{cr},

$$\alpha_{cr}-\alpha = \frac{1}{\sin 2\alpha_{cr}}\left(\frac{T^3}{\rho^3 U_c^4 g}\right)^{1/2}(\kappa_{cr}-\kappa)^2 + O(\kappa_{cr}-\kappa)^3,$$

so that near the critical direction α_{cr}, the directional distribution function of the wave motion is given approximately by

$$\Psi(\alpha) \doteq \frac{\pi\kappa^2\Pi(\boldsymbol{\kappa})t}{\rho^2 U_c^2\cos\alpha}\left(\frac{T}{g^3\rho\sin^2 2\alpha_{cr}}\right)^{1/4}(\alpha_{cr}-\alpha)^{-1/2}. \tag{3.19}$$

The form of $\Psi(\alpha)$ is shown in figure 3. As α increases from zero towards α_{cr}, $\Psi(\alpha)$ increases towards its (integrable) infinity; and when $\alpha > \alpha_{cr}$, $\Psi(\alpha)$ is zero to this approximation.

The mean-square surface displacement is obtained by integrating $\Psi(\alpha)$ over all possible propagation angles α and wave-numbers κ subject to the condition $\chi = 0$. Near $\alpha = \alpha_{cr}$ the directional density of the wave distribution is large and should produce wave patterns more pronounced in this direction than in others. The reason for this accumulation of waves in the direction α_{cr} is, of course, that the range of wave-numbers that propagate at speeds within, say, δc of the minimum speed of surface waves is proportional to $(\delta c)^{1/2}$ only; within an angle $\delta\alpha$ of α_{cr} the range of wave-numbers propagated is proportional to $(\delta\alpha)^{1/2}$, so that the directional density of the wave pattern is proportional to $(\delta\alpha)^{-1/2}$.

The angle between the direction of propagation of these waves and that of the wind, i.e. $\alpha_{cr} = \cos^{-1}(c_{min}/U_c)$, will be small only for light airs. It is doubtful whether a wind of, say, 30 or 40 cm sec^{-1} would contain turbulent components whose scale is as small as the 1·7 cm necessary to excite such waves, and unlikely that they would be observed at small angles α_{cr} under natural conditions. As the wind velocity becomes larger and contains smaller-scale turbulent components, α_{cr} also increases, and these critical angle waves may travel almost at right angles to the wind! Under the conditions visualized in this paper, with a large fetch and sudden onset of the wind, this wave pattern would be a transient one, and would disappear as the waves developed beyond the initial period.

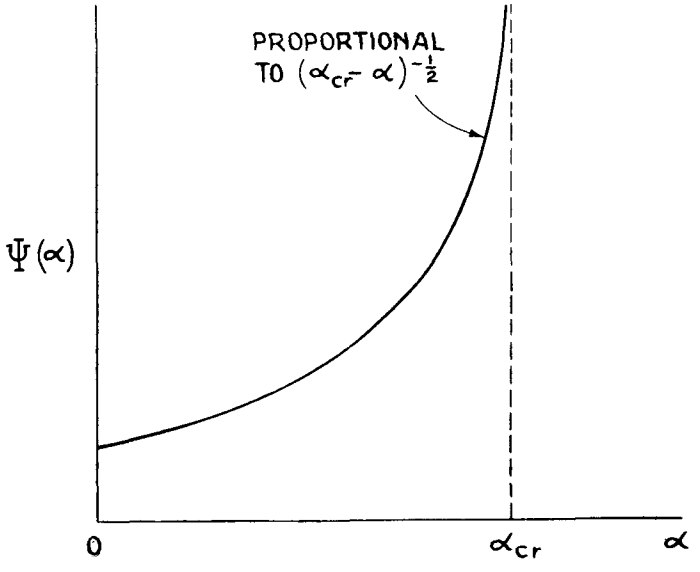

Figure 3.

However, it is likely that the waves are similar to those generated in steady winds at a small fetch, since the time of development of each wave is small, and the growth would be analogous to that discussed here. Assuming a correspondence between the two cases of short wind duration and short fetch, an explanation of some of Roll's (1951) observations can be given. These experiments were made under natural conditions on pools left in tidal mud flats at Neuwerk. On one occasion, when the wind velocity at a height of 35 cm was 195 cm sec^{-1}, Roll observed a rhombic wave pattern of wavelength about 1·7 cm. Unfortunately he does not record the shape of the rhombic pattern, but this observation seems consistent with the establishment of the two trains of resonance waves at angles α_c to the wind direction, as predicted by the theory. On two other occasions, when the wind velocity was approximately 400 cm sec^{-1}, waves

with $\lambda = 1{\cdot}7$ cm were observed with their crests nearly parallel to the direction of the wind, which again is consistent with the theoretical predictions. However, many more careful experiments will have to be made before quantitative comparison with this part of the theory will be possible.

3.3. *The question of* $U_{\min}$

It is perhaps appropriate at this point to offer some remarks concerning the idea that there exists a minimum wind speed capable of raising waves. It is natural that this concept should arise if the problem is considered as one of stability and many attempts to determine $U_{\min}$ experimentally have been made in the past. Ursell (1956), however, discounts the idea, pointing out that any turbulent air motion will necessarily generate some surface displacements, however minute, and that there seems to be no reason why this should not be described as a wave motion. He quotes a table of 'measured values of $U_{\min}$' ranging from 40 cm sec^{-1} (Roll 1951) to above 1200 cm sec^{-1} (Keulegan 1951).

According to the present theory, the minimum wind velocity capable of raising *resonance* waves is 23 cm sec^{-1}, but waves will actually be generated only if there exist near the surface turbulent fluctuations of sufficiently small scale. But, as Ursell points out, turbulent motion in the air will generate surface displacements irrespective of the mean wind velocity. For example, if $U_c = 0$, then in (3.4) $\nu_1 = 0$ and

$$\Gamma = \left(\frac{1-\cos\nu_2}{\nu_2^2}\right)^2, \tag{3.20}$$

so that, when $t < \Theta$,

$$\Phi(\boldsymbol{\kappa}, t) = \frac{\kappa^2 \Pi(\boldsymbol{\kappa})}{\rho^2 n_2^4}(1-\cos n_2 t)^2$$

and

$$\overline{\xi^2} = \frac{1}{\rho^2}\int \frac{\kappa^2\Pi(\boldsymbol{\kappa})}{n_2^4}(1-\cos n_2 t)^2\, d\boldsymbol{\kappa}$$
$$\leqslant \frac{4}{\rho^2}\int \frac{\kappa^2\Pi(\boldsymbol{\kappa})}{n_2^4}\, d\boldsymbol{\kappa} = \text{const.} \tag{3.21}$$

The mean-square displacement of these forced waves is therefore bounded and unlike the resonance waves they do not continue to develop in time. To the eye they may appear as a shimmer or ruffle on an otherwise glassy surface. When $\nu_1 \gg \nu_2$, a similar system of forced oscillations can also be found.

4. The principal stage of development

4.1. *The wave spectral function*

The principal stage of development for a wave-number $\boldsymbol{\kappa}$ is defined as the period during which the time elapsed from the initial instant is greater than $\Theta(\boldsymbol{\kappa})$, the development time of $d\varpi(\boldsymbol{\kappa}, t)$, but not so great that the

amplitude of the wave at this wave-number has increased to such an extent that the infinitesimal wave theory ceases to apply.

We return to the fundamental solution (2.14), namely

$$dA(\boldsymbol{\kappa}, t) = \frac{i\kappa}{2\rho n_2} \int_0^t d\varpi(\boldsymbol{\kappa}, \tau)[\exp\{-i(n_1-n_2)(\tau-t)\} - \\ -\exp\{-i(n_1+n_2)(\tau-t)\}]\, d\tau. \quad (4.1)$$

The wave spectral function $\Phi(\boldsymbol{\kappa}, t)$ is given by

$$\Phi(\boldsymbol{\kappa}, t) = \frac{\overline{dA(\boldsymbol{\kappa}, t)\, dA^*(\boldsymbol{\kappa}, t)}}{d\kappa_1\, d\kappa_2} \\ = \frac{\kappa^2}{4\rho^2 n_2^2} \int_0^t \int_0^t \Pi(\boldsymbol{\kappa}, \tau-\tau')\{\exp\{-i(n_1+n_2)(\tau-\tau')\} + \\ + \exp\{-i(n_1-n_2)(\tau-\tau')\} - 2\exp\{-in_1(\tau-\tau')\}\exp\{-in_2(\tau+\tau')\} \times \\ \times \cos 2n_2 t\}\, d\tau d\tau'. \quad (4.2)$$

If the variables of integration are changed from τ, τ' to τ_1, τ_2, where $\tau_1 = \tau - \tau'$, $\tau_2 = \tau + \tau'$, it is found that the asymptotic form, as $t \to \infty$, of the expression (4.2) is

$$\Phi(\boldsymbol{\kappa}, t) \sim \frac{\kappa^2 t}{4\sqrt{2}\rho^2 n_2^2} \int_{-\infty} \Pi(\boldsymbol{\kappa}, \tau)\{\exp\{-i(n_1+n_2)\tau\} + \exp\{-i(n_1-n_2)\tau\}\}\, d\tau, \quad (4.3)$$

where the suffix has now been dropped from τ_1. This asymptotic form can be written in a simpler manner if we interpret the integral in terms of time scales in frames of reference themselves moving with respect to the convected frame in which the analysis has been made. If a spatial Fourier transform $F(\boldsymbol{\kappa}, \tau)$ of some covariance $f(\mathbf{r}, \tau)$, a function of space separation $\mathbf{r}$ and time interval τ, is defined as

$$f(\mathbf{r}, \tau) = \int F(\boldsymbol{\kappa}, \tau) e^{i\boldsymbol{\kappa} \cdot \mathbf{r}}\, d\boldsymbol{\kappa},$$

then, in a reference frame moving with a relative velocity $\mathbf{V}$, such that $\mathbf{r} = \mathbf{q} + \mathbf{V}\tau$, we have

$$f(\mathbf{q}, \tau) = \int F(\boldsymbol{\kappa}, \tau) e^{i(\boldsymbol{\kappa} \cdot \mathbf{q} + \boldsymbol{\kappa} \cdot \mathbf{V}\tau)}\, d\boldsymbol{\kappa},$$

so that

$$e^{i\boldsymbol{\kappa} \cdot \mathbf{V}\tau} F(\boldsymbol{\kappa}, \tau) = (2\pi)^{-2} \int f(\mathbf{q}, \tau) e^{-i\boldsymbol{\kappa} \cdot \mathbf{q}}\, d\mathbf{q},$$

the $\mathbf{q}$-coordinates being in the moving frame of reference. Thus the spectral function in the moving frame is

$$e^{i\boldsymbol{\kappa} \cdot \mathbf{V}\tau} F(\boldsymbol{\kappa}, \tau),$$

where $F(\boldsymbol{\kappa}, \tau)$ is the spectral function in the original frame. The integral time scale, for the wave-number $\boldsymbol{\kappa}$, in the moving frame, is therefore given by $\theta(\boldsymbol{\kappa}, \mathbf{V})$, where

$$\int_{-\infty}^{\infty} e^{i\boldsymbol{\kappa} \cdot \mathbf{V}\tau} F(\boldsymbol{\kappa}, \tau)\, d\tau = 2F(\boldsymbol{\kappa}, 0)\theta(\boldsymbol{\kappa}, \mathbf{V}). \quad (4.4)$$

Equation (4.3) can therefore be expressed as

$$\Phi(\boldsymbol{\kappa}, t) \sim \frac{\kappa^2 \Pi(\boldsymbol{\kappa}, 0) t}{2\sqrt{2}\rho^2 n_2^2} \{\theta(\boldsymbol{\kappa}, V_1) + \theta(\boldsymbol{\kappa}, V_2)\}, \tag{4.5}$$

where, from (4.4), V_1 and V_2 are given by

$$\left.\begin{aligned} -\boldsymbol{\kappa} \cdot \mathbf{V}_1 = n_1 + n_2 = \boldsymbol{\kappa} \cdot \mathbf{U}_c + (g\kappa + T\kappa^3/\rho)^{1/2}, \\ -\boldsymbol{\kappa} \cdot \mathbf{V}_2 = n_1 - n_2 = \boldsymbol{\kappa} \cdot \mathbf{U}_c - (g\kappa + T\kappa^3/\rho)^{1/2}, \end{aligned}\right\} \tag{4.6}$$

so that

$$\boldsymbol{\kappa} \cdot (\mathbf{U}_c + \mathbf{V}_1) = -\kappa c(\kappa), \qquad \boldsymbol{\kappa} \cdot (\mathbf{U}_c + \mathbf{V}_2) = \kappa c(\kappa), \tag{4.7}$$

$c(\kappa)$ being, as before, the speed of free surface waves of wave-number κ. Notice that the velocities $\mathbf{V}$ (relative to the convected frame) of the frames of reference in which the time scales are to be measured are each specified by only one scalar equation, so that either the speed V of this frame, or its direction of motion can be chosen arbitrarily. For convenience the direction of $\mathbf{V}$ can be chosen to coincide with that of $\mathbf{U}$, and so

$$(U_c + V_1)\cos\alpha = -c(\kappa), \qquad (U_c + V_2)\cos\alpha = c(\kappa).$$

Hence $$V_1 = -U_c - c(\kappa)/\cos\alpha, \qquad V_2 = -U_c + c(\kappa)/\cos\alpha. \tag{4.8}$$

The absolute speeds of the frames of reference in which the scales θ are to be measured are $c(\kappa)/\cos\alpha$ and $-c(\kappa)/\cos\alpha$, the negative sign implying motion in the direction against the wind. It is evident that the time scale of the pressure fluctuations observed in a reference frame moving against the wind is less than that moving with the wind at the same speed, so that $\theta(\boldsymbol{\kappa}, V_1) \ll \theta(\boldsymbol{\kappa}, V_2)$, and the expression (4.5) can be approximated by

$$\Phi(\boldsymbol{\kappa}, t) \sim \frac{\kappa^2 \Pi(\boldsymbol{\kappa}) t}{2\sqrt{2}\rho^2 n_2^2} \theta(\boldsymbol{\kappa}, V). \tag{4.9}$$

The speed $V = c(\kappa)/\cos\alpha$ is just equal to that of the waves of wave-number κ propagating in the direction α, observed along a line parallel to the wind, so that the integral time scale represents the time scale of the variations in phase difference between the pressure fluctuations and the wave pattern.

The expression (4.9) is the basic result of this part of the paper, and from it several important deductions can be made immediately. Since the only way in which the elapsed time t enters the right-hand side is in the explicit linear factor, the mean-square wave height is directly proportional to time in the principal stage of development. Furthermore, the shape of the wave spectrum is independent of time, at any rate until the development is such that the mean-square slope (governing the importance of non-linearities in the equation of motion) associated with any group of wave-numbers becomes too large. It will be seen later that this occurs first at the shorter wavelengths excited, and the contribution from these to the total mean-square surface displacement is small. Thus the direct proportionality of $\overline{\xi^2}$ to t should continue until the mean-square slope of the largest waves attains a limiting value, after which time an equilibrium structure is presumably attained.

However, a direct application of (4.9) is hindered by the presence of the factor $\theta(\boldsymbol{\varkappa}, V)$ about which little is known. When $V = U_c$, so that the wave pattern moves with the convection velocity of the pressure fluctuations, we have the true resonance waves which figured in § 3.2, and the time scale $\theta(\boldsymbol{\varkappa}, V)$ is equal to the convected or natural time scale Θ. The use of the capital letter in this latter case emphasizes the particular significance of this time scale. However, when $V \neq U_c$, and usually $V < U_c$, the time scale in the reference frame moving with speed V is less than Θ, since it is governed by the rate at which the convected fluctuations are swept past the point of observation. A rough approximation to $\theta(\boldsymbol{\varkappa}, V)$, but one which is probably satisfactory, is to take it as the length scale κ^{-1} divided by the relative speed of the convected pressure fluctuations and the waves; thus

$$\theta(\boldsymbol{\varkappa}, V) \doteqdot \frac{1}{\kappa(U_c - c(\kappa)/\cos\alpha)}, \tag{4.10}$$

when U_c is greater by about a factor of about two than $c(\kappa)/\cos\alpha$. More properly, the time scale represented by the expression on the right is a differential scale, whereas $\theta(\boldsymbol{\varkappa}, V)$ is defined as an integral scale. However, the two scales should be proportional, and probably of the same order of magnitude, so that the approximation (4.10) can be used in the absence of better information, provided the results are interpreted as being valid only to orders of magnitude.

For gravity waves, $n_2^2 = g\kappa$, so that, from (4.9) and (4.10), we have

$$\Phi(\boldsymbol{\varkappa}, t) \sim \frac{\Pi(\boldsymbol{\varkappa})t}{2\sqrt{2\rho^2 g(U_c - c(\kappa)/\cos\alpha)}}. \tag{4.11}$$

When U is greater than $c(\kappa)/\cos\alpha$ by a factor of about three or four, this expression can be further simplified to

$$\Phi(\boldsymbol{\varkappa}, t) \sim \frac{\Pi(\boldsymbol{\varkappa})t}{2\sqrt{2\rho^2 U_c g}}, \tag{4.12}$$

so that we have immediately

$$\boxed{\overline{\xi^2} \sim \frac{\overline{p^2}t}{2\sqrt{2\rho^2 U_c g}}}, \tag{4.13}$$

and, for the mean-square slope,

$$\overline{(\nabla\xi)^2} \sim \frac{\overline{(\nabla p)^2}t}{2\sqrt{2\rho^2 U_c g}}. \tag{4.14}$$

Further reference will be made presently to these particularly simple and important results. At this stage we must consider the conditions under which the assumption that $U_c \gg c(\kappa)/\cos\alpha$ is likely to be valid for most of the range of wave-numbers over which the spectral function $\Phi(\boldsymbol{\varkappa})$ is significant. Support is given to the approximation (4.10) by the observation that for moderate winds over all but the longest durations, the wave spectrum is appreciable only over wave-numbers for which the condition $U_c \gg c(\kappa)$ is satisfied. It is instructive, however, to see why this

is so by examining the relevant meteorological and other evidence on the surface pressure fluctuations. The dependence of this function on $\boldsymbol{\kappa}$ is determined, as (4.9) shows, jointly by $\theta(\boldsymbol{\kappa}, V)$ and the pressure term, which for gravity waves where $n_2^2 = g\kappa$ is of the form $\kappa\Pi(\boldsymbol{\kappa})$. It is unfortunate that the properties of the spectral function $\Pi(\boldsymbol{\kappa})$ of the imposed surface pressure distribution are at present almost unknown, though by using the results of some recent atmospheric measurements of the turbulent velocities (made over land, alas, not over the sea), some of its qualitative properties can be surmised. But one important property that can be established without recourse to these experiments is that when $\boldsymbol{\kappa} = 0$, $\Pi(\boldsymbol{\kappa}) = 0$; this is proved

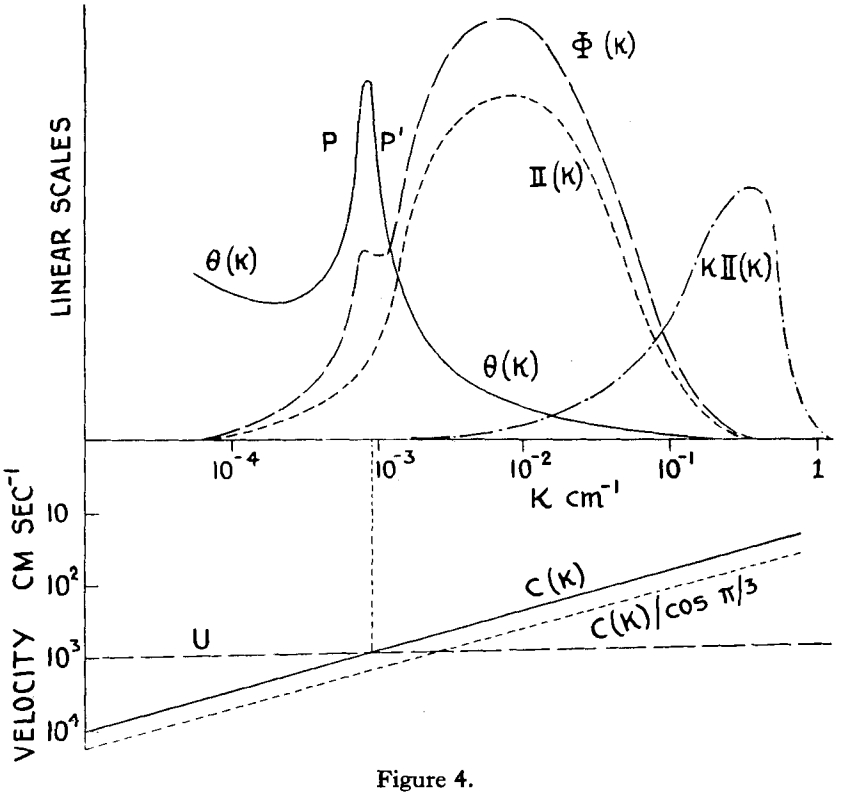

Figure 4.

in the Appendix to this paper. Thus in any direction α in the κ-plane, $\Pi(\boldsymbol{\kappa})$ rises from zero at the origin to a maximum and then decreases again to zero as κ approaches its value for the dissipating eddies. We are now faced with the question of deciding the order of magnitude of the values of κ for which $\Pi(\boldsymbol{\kappa})$ is a maximum. The only guide we have at present are experiments such as those of MacCready (1953 a, b), Taylor (1955) and Ellison (1956) on velocity autocorrelations over land in winds within the range 1 to 5 m sec^{-1}. These point to a longitudinal scale of the energy-containing eddies in the lowest few metres of the order 10 m (the lateral

scales are considerably smaller), that is to say, the peak value of the velocity spectrum under these conditions occurs at wave-numbers of order $2\pi/10^3 = 6 \times 10^{-3}$ cm^{-1}. Apparently this scale does not depend greatly upon wind velocity or distance from the ground. In isotropic turbulence, Batchelor (1951) has shown that the scale of the pressure fluctuations is rather less, about half, of that of the velocity fluctuations; and if a similar situation exists in the atmosphere, the maximum value of $\Pi(\boldsymbol{\kappa})$ may occur for values of κ of about 10^{-2} cm^{-1}. Furthermore, atmospheric turbulence generally contains a large range of eddy sizes, so that the spectra tend to be fairly broad. These considerations make it likely that $\Pi(\boldsymbol{\kappa})$, in a given direction α in the κ-plane, is a function of κ of the shape illustrated in the top portion of figure 4, with a broad maximum near $\kappa = 10^{-2}$ cm^{-1}, decreasing to zero for both large and small values of κ. The function $\kappa\Pi(\boldsymbol{\kappa})$, being weighted towards the larger values of κ, has its maximum at a larger κ, and would be expected to be of the form also illustrated in figure 4.

The time scale $\theta(\boldsymbol{\kappa})$ has its maximum when κ has such a value that the waves of this wave-number move with the convection velocity U_c; then $\theta(\boldsymbol{\kappa}) = \Theta$, the development time of the pressure fluctuations. For a wind speed of, say, 10^3 cm sec^{-1}, a fresh sailing breeze, the maximum for angles α in the range $-\frac{1}{3}\pi$ to $\frac{1}{3}\pi$ (containing most of the wave energy) occurs when $\kappa \sim 10^{-3}$ cm^{-1}. For larger and smaller values of κ away from this maximum, $\theta(\boldsymbol{\kappa})$ is given by (4.10), so that the function has the form of the solid curve in the upper part of figure 4.

The wave spectrum is given by the product of the functions $\theta(\kappa)$ and $\kappa\Pi(\boldsymbol{\kappa})$ represented by the curves in this diagram, and it is clear that for a wind speed of 10 m sec^{-1} the range of wave-numbers PP', over which the approximation (4.10) is insufficient, contributes little to the integral $\int \Phi(\boldsymbol{\kappa})\, d\boldsymbol{\kappa}$. The result (4.12), therefore, would be expected to give a good approximation to the wave spectrum except for the smallest values of κ, whose contribution to the mean-square wave height is small. For wind speeds greater than the value 10^3 cm sec^{-1} chosen for purposes of illustration in figure 4, the wave-number for which $U_c = c(\kappa)$ decreases as U^{-2}, so that the curve $\theta(\boldsymbol{\kappa})$ is translated to the left. It is unlikely that the reciprocal of the scale of the pressure-generating eddies should decrease with wind speed as rapidly as this, so that the range of wave-numbers PP' contributes even less to the integrated wave spectrum, and the approximations inherent in (4.12) and (4.13) become more accurate. However, when the wind speed and associated convection velocity is small, say 1 m sec^{-1}, it is probable that the range PP' will occur at a point where the value of $\kappa\Pi(\boldsymbol{\kappa})$ is no longer negligible. These circumstances are illustrated in figure 5, and the wave spectrum calculated from the curves $\theta(\boldsymbol{\kappa})$ and $\kappa\Pi(\boldsymbol{\kappa})$ is clearly no longer similar in shape to $\Pi(\boldsymbol{\kappa})$ but possesses a more pronounced peak. In light winds, therefore, the wave spectrum is narrower, and presumably the wave pattern more regular, a deduction which would appear to be substantiated by visual observations. A similar situation exists for higher wind velocities when α is very nearly $\pm\frac{1}{2}\pi$, and the curve $\theta(\boldsymbol{\kappa})$ is displaced considerably to the right, but the

range of angles over which the approximation (4.10) fails is small and again contributes little to the integrated wave spectrum, or to $\overline{\xi^2}$.

4.2. *Termination of the principal stage of development*

There is another effect which limits the validity of (4.12) and (4.13) and which we have not yet considered. As the wave pattern develops, the mean-square slope of the waves increases linearly with time. After a certain interval, the mean-square slope associated with some band of wave-numbers becomes so large that the waves can no longer be described by a linear

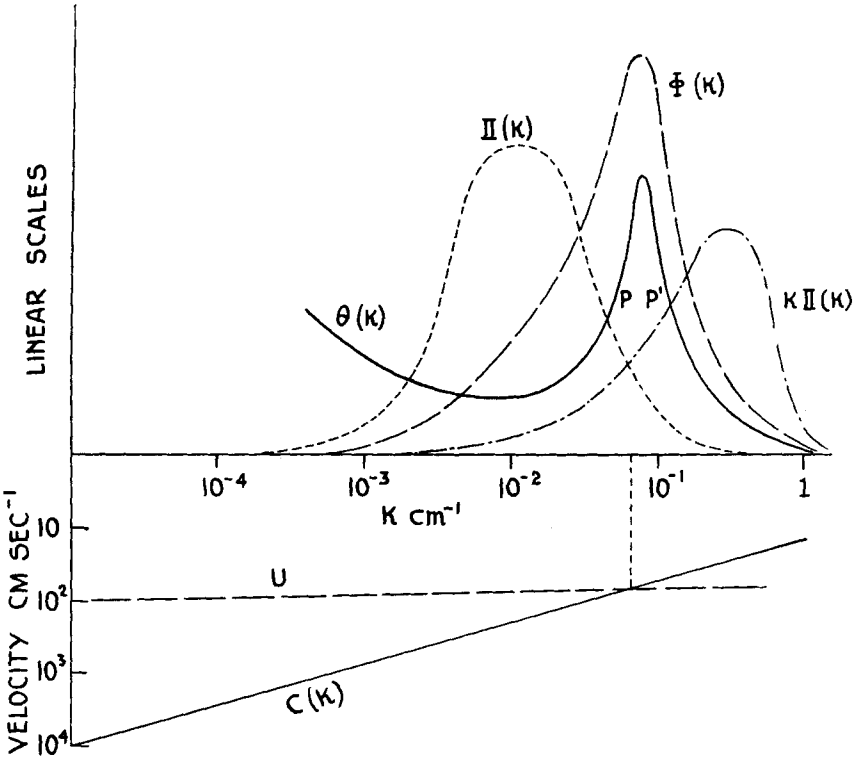

Figure 5.

theory. The non-linear processes which then become important tend, among other things, to limit the maximum surface slope that can be attained. Without a detailed examination of the role of the non-linearities in modifying the wave spectrum, it is not immediately clear exactly what criterion determines the importance of the non-linearities, although it is very reasonable to suppose that it concerns the value of the slope spectrum $\kappa^2\Pi(\boldsymbol{\kappa})$ in some manner. There is some evidence (Danel 1956) that the effect is appreciable when the mean-square surface slope $\overline{(\nabla\xi)^2} = \int\kappa^2\Phi(\boldsymbol{\kappa})\,d\boldsymbol{\kappa}$ attains a certain value. But whatever the exact criterion might be, provided only that it involves a limitation on the slope spectrum, which is largest when the wave-number κ is large or the wavelength λ small, its effect will

clearly be felt first in this range of κ; the actual wave spectrum will for these wave-numbers be smaller than that predicted by the linear theory, and instead of continuing to grow will presumably attain some sort of equilibrium. As time goes on and the wave amplitudes at other wave-numbers increase, the wave-numbers contributing significantly to the slope spectrum extend to smaller and smaller values; so that the effects of the non-linearity gradually spread to the wave-numbers for which the wave spectrum $\Phi(\boldsymbol{\kappa})$ itself is appreciable. This process whereby the principal stage of development of each wave-number is ended in turn implies that the value of λ for which $\Phi(\boldsymbol{\kappa})$ is a maximum increases with time, since the longer waves continue to grow while the amplitude of the shorter waves is limited. A detailed analytical description of this process has not yet been attempted, but it seems likely to provide part of the explanation of the observed increase with time in the dominant wavelength of the surface displacement.

An important consequence of these remarks is that the result (4.13) remains valid until the wave-numbers near the maximum of the linear spectrum $\Phi(\boldsymbol{\kappa})$ become affected by the non-linearity, although over a large range of larger wave-numbers, or smaller wavelengths, the principal stage of development has terminated, and the expression (4.14) for the mean-square slope has become seriously inadequate. The reason is, of course, that the wave-numbers contributing greatly to the slope spectrum make little contribution to the wave spectrum.

4.3. *Comparison with observations on the wave field*

The most important result of §4.2 from the practical point of view is (4.13). In order to compare this result with the oceanographic measurements that are available for conditions of finite duration, we must obtain an estimate for $\overline{p^2}$ in terms of the quantities that determine the mean velocity profile of the wind. It has already been pointed out that these relevant parameters are the friction velocity u_* and (for aerodynamically rough flow) the length z_0, so that the mean-square pressure fluctuations at the surface should be expressed as

$$\overline{p^2} = A\rho_a^2 u_*^4, \tag{4.15}$$

where A is a numerical constant to be estimated and ρ_a is the density of the air.

In shear-flow turbulence in general, $\overline{p^2}$ is of the order of $\frac{1}{4}\rho_a^2 \overline{\mathbf{v}^2} V^2$, where $\mathbf{v}$ and V are turbulent and mean velocities representative of the region concerned. The atmospheric measurements of MacCready (1953 b) are helpful in applying this expression and obtaining an estimate for A. Under conditions of almost neutral thermal stability over land with z_0 of the order 0·1 cm, he found that in the lowest few metres $\overline{\mathbf{v}^2} = \overline{v_1^2} + \overline{v_2^2} + \overline{v_3^2} \doteq \frac{1}{4}V^2$. In view of the fact that under these conditions, the maximum of the pressure spectrum occurs at wave-numbers corresponding to length scales of order 10 m, it seems likely that the velocity fluctuations at heights of the order of 1 m contribute most to $\overline{p^2}$, and by relating MacCready's measured

values of $\overline{\mathbf{v}^2}$, V and u_*, we obtain the result that, to the correct order of magnitude at least,

$$\overline{p^2} \doteq 9 \times 10^3 \rho_a^2 u_*^4. \tag{4.16}$$

In most published oceanographic measurements, the wave heights observed have been expressed in terms of wind velocities U measured at some level, usually several metres, from the surface. In order to compare our theory with these observations, it is necessary to relate the friction velocity to the measured 'wind velocity' for conditions similar to those under which the observations were made. For the sea surface with moderate winds, a typical value of z_0 is of the order of 0·15 cm, and if the height z at which U is observed is of the order of 5 m, we have from (2.1) that approximately

$$U \doteq 18 u_*.$$

The factor 18 is not critically dependent upon z or z_0, so that it can reasonably be taken as representative of the conditions under which measurements, such as those reported by Sverdrup & Munk (1947), were made. From (4.16), therefore

$$\overline{p^2} \doteq 9 \times 10^{-2} \rho_a^2 U^4.$$

This relation can be substituted into (4.13), and since for pressure components of the scale of gravity waves the convection velocity U_c is equal to the velocity several metres from the surface, it is approximately equal to the 'wind velocity' U. We therefore have, from (4.13),

$$\overline{\xi^2} \sim 0{\cdot}035 \left(\frac{\rho_a}{\rho_w}\right)^2 \frac{U^3 t}{g}.$$

where ρ_w is the density of the water.

In oceanographic practice, wave heights are usually measured from trough to crest, and a widely used measure is H, the mean height of the third highest waves. Longuet-Higgins (1952) has shown that $H^2 = 8\overline{\xi^2}$ approximately, so that the previous equation can be written

$$\frac{gH}{U^2} \sim 6 \times 10^{-4} \left(\frac{gt}{U}\right)^{1/2}, \tag{4.17}$$

taking the value 10^{-3} for ρ_a/ρ_w. The accuracy of the constant in this expression is quite low, mainly as a result of the uncertainties in the value of $\overline{p^2}$ to be expected upon the surface. (Some reliable measurements of this would be very valuable.) It might be pointed out, however, that the factor $2^{-3/2}$ in (4.13) represents an underestimate in consequence of the neglect of $\theta(\mathbf{\kappa}, V_1)$ and of the term $c(\kappa)/\cos\alpha$ in (4.11) leading to (4.12).

When the result (4.17) is compared with some of the wave heights observed under conditions of finite duration as in figure 6, we find quite good agreement over the rather restricted range of durations for which measurements have been made. The observations are those given by Sverdrup & Munk in their figure 7. The ratios of the speed C of the highest waves to the wind speed U are also plotted in figure 6, and in these

observations the ratio C/U is of the order of unity. Under these circumstances, other wave-generating processes such as sheltering and the effects of variations in shear stresses may have become important, and, in any case, this theory would be expected to give an appreciable underestimate of the wave heights for the reasons mentioned above. In spite of this, it seems that the approximations used are sufficiently accurate to account for the order of magnitude of the wave heights observed.

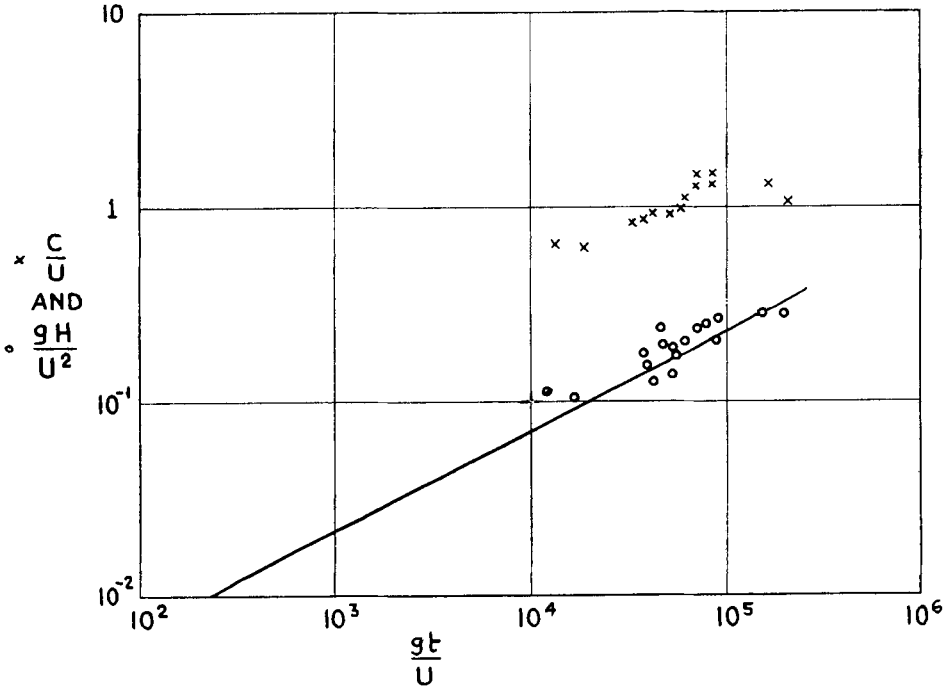

Figure 6.

We are now in a position to see rather more clearly the probable reason for the failure of Eckart's theory to predict the magnitude of the wave heights generated by the wind. His less precise specification of the pressure distribution has 'smoothed off' the resonance peak of the response of the water surface, and it is the wave-numbers near this peak that can contribute largely to the wave spectrum at large durations.

Appendix

We wish to show that $\Pi(\boldsymbol{\varkappa}) = 0$ when $\boldsymbol{\varkappa} = 0$, or equivalently that

$$\int \overline{p(\mathbf{x})p(\mathbf{x}+\mathbf{r})}\, d\mathbf{r} = 0,$$

the integration being over the whole surface with $\mathbf{x}$ fixed. This result is established by joint consideration of the surface boundary condition (2.12)

relating the surface displacements to the surface pressure distribution, and the dynamics of the mass of air above. If (2.12) is multiplied in turn by $dA''(\boldsymbol{\kappa}, t)$ and $d\varpi(\boldsymbol{\kappa}, t)$, and the probability average taken to find the spectral functions in the manner of (2.3), we can put $\boldsymbol{\kappa} = 0$ (and so $n_1 = n_2 = 0$) in the resulting equations. The result of these operations can be expressed as

$$\int \overline{\ddot{\xi}(\mathbf{x})\ddot{\xi}(\mathbf{x}+\mathbf{r})}\, d\mathbf{r} = 0,$$

$$\int \overline{p(\mathbf{x})\ddot{\xi}(\mathbf{x}+\mathbf{r})}\, d\mathbf{r} = 0,$$

or if v_3 is the velocity of the fluid normal to the surface Σ, say,

$$\left.\begin{aligned} \int \overline{\dot{v}_3(\mathbf{x})\dot{v}_3(\mathbf{x}+\mathbf{r})}\, d\Sigma(\mathbf{r}) = 0, \\ \int \overline{p(\mathbf{x})\dot{v}_3(\mathbf{x}+\mathbf{r})}\, d\Sigma(\mathbf{r}) = 0. \end{aligned}\right\} \tag{A.1}$$

We now turn to the dynamics of the fluid above the liquid surface. It has been proved formally by the author in another context (Phillips 1956) that the integrated surface pressure covariances are related to the acceleration covariances, integrated throughout the fluid, by an expression of the form

$$\int \overline{g(\mathbf{x})p(\mathbf{x}+\mathbf{r})}\, d\Sigma(\mathbf{r}) = \rho_a \int \overline{g(\mathbf{x})\dot{v}_3(\mathbf{x}+\mathbf{r}')}\, d\mathbf{r}', \tag{A.2}$$

where $\mathbf{r}' = r_1', r_2', r_3'$ is a point in the interior of the fluid, and the integration on the right is throughout the volume occupied by the fluid. $g(\mathbf{x})$ is a fluctuating quantity of zero mean whose precise nature is, in this expression, immaterial; it is introduced simply to provide integrable covariances with $p(\mathbf{x}+\mathbf{r})$ and $\dot{v}_3(\mathbf{x}+\mathbf{r})$. Taking $g(\mathbf{x}) = p(\mathbf{x})$, the surface pressure at the point $\mathbf{x}$, it can be shown to be a consequence of continuity that

$$\iint \overline{p(\mathbf{x})\dot{v}_3(\mathbf{x}+\mathbf{r}')}\, dr_1' dr_2'$$

is independent of r_3'. But when $r_3' = 0$, i.e. at the surface, this integral vanishes according to (A.1) so that the integral

$$\iiint \overline{p(\mathbf{x})\dot{v}_3(\mathbf{x}+\mathbf{r}')}\, dr_1' dr_2' dr_3'$$

vanishes throughout any layer of large finite thickness above the surface. Hence, from (A.2),

$$\int \overline{p(\mathbf{x})p(\mathbf{x}+\mathbf{r})}\, d\Sigma(\mathbf{r}) = 0, \tag{A.3}$$

which is the result that we set out to establish.

References

Batchelor, G. K. 1951 *Proc. Camb. Phil. Soc.* **47**, 359.

Batchelor, G. K. 1953 *The Theory of Homogeneous Turbulence.* Cambridge University Press.

Danel, P. 1956 *Proc. IV Journées de l'Hydraulique* (Paris).

Eckart, C. 1953 *J. Appl. Phys.* **24**, 1458.

Ellison, T. H. 1956 *Surveys in Mechanics*, p. 400. Cambridge University Press.

Jeffreys, H. 1924 *Proc. Roy. Soc.* A, **107**, 189.

Jeffreys, H. 1925 *Proc. Roy. Soc.* A, **110**, 341.

Keulegan, G. H. 1951 *J. Res. Nat. Bur. Stand., Wash.*, **50**, 99.

Longuet-Higgins, M. S. 1952 *J. Mar. Res.* **11**, 245.

MacCready, P. B. 1953 a *J. Met.* **10**, 325.

MacCready, P. B. 1953 b *J. Met.* **10**, 434.

Phillips, O. M. 1955 *Proc. Camb. Phil. Soc.* **51**, 220.

Phillips, O. M. 1956 *Proc. Roy. Soc.* A, **234**, 327.

Roll, H. U. 1951 *Ann. Met.* (*Hamburg*) **4**, 269.

Sverdrup, H. U. & Munk, W. 1947 *Wind, Sea and Swell. Theory of Relations for Forecasting. Publ. Hydrog. Off., Wash.*, no. 601.

Taylor, R. J. 1952 *Quart. J. Roy. Met. Soc.* **78**, 179.

Taylor, R. J. 1955 *Aust. J. Phys.* **8**, 535.

Ursell, F. 1956 *Surveys in Mechanics*, p. 216. Cambridge University Press.